

Control Strategies and Inverter Topologies for Stabilization of DC Grids in Embedded Systems

Nicolas Patin, The Dung Nguyen, Guy Friedrich

June 12, 2009

Keywords

PWM strategies, Converter topologies, Embedded systems, DC grid stability, Uncertain/Varying parameters.

Abstract

Compactness is a key constraint for embedded equipments design. The main issue concerns DC link capacitors, which must maintain a good DC voltage quality. However, their size is too high when classical PWM strategies are used. In this paper, two adapted techniques are compared with uncertain or varying grid parameters.

1 Introduction

During the last decade, electric and hybrid vehicles have been significantly studied by manufacturers (e.g. Toyota Prius) and academic institutions [1]. As a consequence, integration of power electronics converters (here, a PWM inverter as shown in Fig. 1) is more and more difficult mainly because of passive components that are usually the most cumbersome in such systems. Extensive studies have been already carried out about reduction of DC link capacitors by using adapted PWM control strategies [2]. However, in this previous study, reduction of DC capacitor value is only based on a reduction of i_{dc} RMS value without taking into account the grid impedance. It can be shown that, if capacitor value is reduced enough, the stability of DC bus voltage cannot be guaranteed. Indeed, a parallel resonance can occur between DC bus capacitors (C_{dc}) and grid inductance (L_g) if i_{dc} spectrum contains harmonic components close to the resonance frequency $\omega_r = 1/\sqrt{L_g \cdot C_{dc}}$.

Thus, input current spectrum must be controlled but resonance frequency is not exactly known because, as it is shown in section 2, on one hand, there is a large uncertainty of the grid inductance value for small geometry variations of cable placement in the vehicle frame and on the other hand, in a complex grid with several interconnected converters, significant variations of the grid impedance can be observed. So, the Pulse Width Modulation (PWM) strategy applied to the inverter must bring good performances with a sufficient robustness against parameters uncertainties and/or variations.

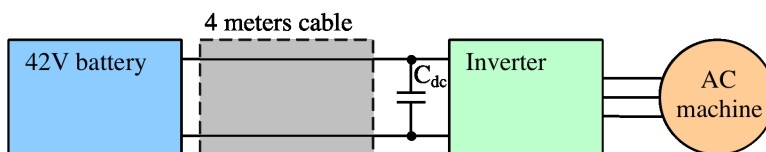


Figure 1: Minimal structure of a DC grid in embedded systems (e.g. Hybrid vehicle)

For this purpose, the impact of a Random Carrier Frequency PWM [3] control strategy is studied in section 3. Then, a modified converter (three-phase four legged inverter) [4] controlled with a large bandwidth zero-sequence current regulation loop is used for DC bus stabilization in section IV. Performances will be compared in order to evaluate the interest of changing converter topology in terms of compactness of the global system.

2 Modeling

The minimal structure studied in this paper is presented in Fig. 1. It includes a battery, a 4 meter cable (2 conductors) that corresponds to a minimal DC grid in embedded systems and an inverter supplying an AC load (a permanent magnet synchronous motor for instance). Obviously, this topology with a long DC bus cable is not physically satisfactory but it cannot always be avoided in specific applications because of various technical constraints. In such cases, alternative filtering solutions should be applied in order to fulfill specifications under classic embedded systems constraints (compactness and high reliability).

2.1 Inverter

The inverter is modeled using ideal switches:

- voltage drops are neglected
- Instantaneous turn-on and turn-off, without dead time

For the classical three-legged inverter, the load, connected to the AC terminals of the inverter is supposed to be balanced. Thus, zero sequence voltage is equal to zero. So, it yields to

$$v_a + v_b + v_c = 0 \quad (1)$$

And then, voltage vector, noted $(v_3) = (v_a, v_b, v_c)^t$ can be expressed as follows

$$(v_3) = \frac{v_{dc}}{3} \begin{pmatrix} 2 & -1 & -1 \\ -1 & 2 & -1 \\ -1 & -1 & 2 \end{pmatrix} \cdot (Sw_3) \quad (2)$$

where $(Sw_3) = (Sw_a, Sw_b, Sw_c)^t$ is the switching function vector. Equation (2) must be associated to the corresponding current equation:

$$i_{dc} = (Sw_3)^t \cdot (i_3) \quad (3)$$

On the basis of (1) and (2), it can be seen that the instantaneous input power equals to the output one. Obviously, an average model can be derived from these two instantaneous equations by replacing switching functions with their average values (on a T_s time window - T_s being the switching period), namely as *duty ratios* α_a , α_b and α_c .

2.2 Grid uncertainties

The grid model is limited to the simplest structure using only one converter connected to the battery using two conductors. In practice, these two conductors are isolated from the vehicle frame as indicated in Fig. 2a.

Finite element simulations (using FEMM 4.2 software - see Fig. 2b.) have been performed in order to evaluate the inductance of this cable for different values of the two geometrical parameters defined as follows:

- Distance H between vehicle frame/conductor,

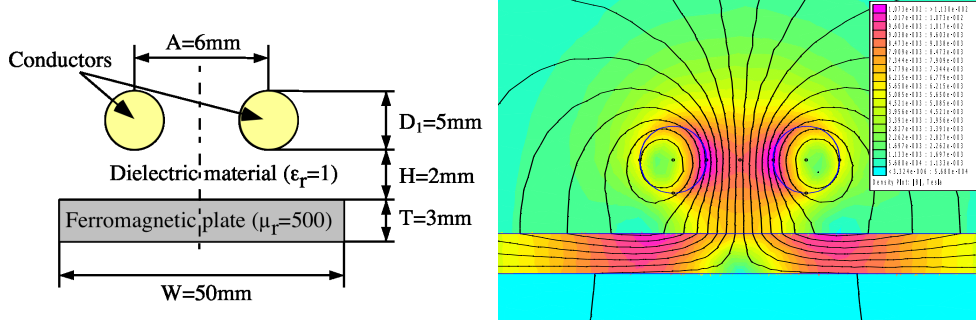


Figure 2: Grid geometry (a: left) and FE simulation (b: right)

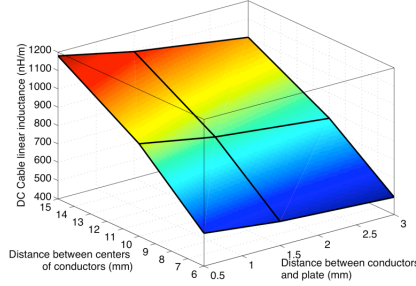


Figure 3: DC grid linear inductance variation

- Distance A between centers of the two conductors.

Simulation results indicate that realistic A and H variations (from a vehicle electric network to another one) lead to inductance variation of more than 140% (see Tab. 1 and Fig. 3 : from 495nH/m to 1,18 μ H/m). Moreover, in a more complex grid (*i.e.* with several interconnected inverters), parallel converters and their loads modify the impedance of the grid.

Table 1: Nominal DC grid parameters values

Parameters	Value	Unit
Conductors diameter D_1	5	mm
Distance A between centers of conductors	6	mm
Distance H between conductors and plate	2	mm
Plate width W	50	mm
Plate thickness	3	mm
Relative permittivity of insulators ϵ_r	1	/
Relative permeability of iron alloy plate μ_r	500	/

2.3 Impact of parallel drives

The impedance of the DC grid can be modified by other drives connected to the bus. Indeed, it is possible to calculate the equivalent DC bus impedance of converter connected to a three-phase load and this parallel impedance can vary with the operating point of the converter (For instance, an inverter connected to a three-phase RL series load):

$$(v_3) = R. (i_3) + L \frac{d}{dt} (i_3)$$

where (v_3) is controlled by the inverter according to Eq. 5. Thus

$$(i_3) = \frac{v_{dc}}{3 \cdot (R + Ls)} \begin{pmatrix} 2 & -1 & -1 \\ -1 & 2 & -1 \\ -1 & -1 & 2 \end{pmatrix} \cdot (Sw_3)$$

where s is the Laplace transform variable. And finally, using Eq. 3, it gives

$$i_{dc} = \frac{v_{dc}}{3 \cdot (R + Ls)} (Sw_3)^t \begin{pmatrix} 2 & -1 & -1 \\ -1 & 2 & -1 \\ -1 & -1 & 2 \end{pmatrix} \cdot (Sw_3)$$

As a consequence, the equivalent admittance of the system can be derived from this equation replacing switching functions vector (Sw_3) by their average values, namely as duty ratios vector (α_3) . Thus it gives

$$Y_{eq}(s) = \frac{1}{3(R + Ls)} (\alpha_3)^t \cdot \begin{pmatrix} 2 & -1 & -1 \\ -1 & 2 & -1 \\ -1 & -1 & 2 \end{pmatrix} \cdot (\alpha_3) \quad (4)$$

In steady-state operation (with sinusoidal duty ratios¹), it gives

$$Y_{eq}(s) = \frac{3k_m^2}{8} \cdot \frac{1}{R + Ls} \quad \text{where } 0 \leq k_m \leq 1 \quad (5)$$

3 Random Carrier Frequency PWM

The proposed strategy is a classical Random Carrier Frequency PWM technique with a given random distribution of the switching frequency F_d . For a uniform distribution of F_d in a bounded set $[F_{av} + \delta F/2, F_{av} - \delta F/2]$, It can be seen in Fig. 4 that spread spectrum occurs when normalized frequency deviation $\delta F/F_{av}$ increases (from 0 to 0.4 with average switching frequency $F_{av} = 10\text{kHz}$). As a consequence, disturbances are spread over a large bandwidth reducing resonance excitation for a given couple (L_g, C_{dc}) .

However, even if amplitudes are reduced, harmonics cannot be neglected and if the damping coefficient is too small, resonance induced on the dc voltage can be destructive (see Fig. 5). Moreover, this technique is not robust against parameters variations. Indeed, as it has been shown in section 2 that, the grid impedance can vary because of parallel converters. So, an closed loop control should be preferred in order to avoid varying parameters issues.

4 DC grid voltage stabilization using a four-legged inverter

4.1 Predictive hybrid control principles

If the switching frequency cannot be increased enough due to of the limitations introduced by thermal constraints and switching losses, spread spectrum brought by RCF PWM (or other random PWM techniques) is not sufficient. Thus, other solutions must be investigated. The one proposed in this paper is based on a three-phase four-legged inverter (Fig. 7). In such a converter, it is possible to control the zero-sequence current i_{zs} independently from $\alpha\beta$ ones. In this study, a hybrid predictive controller is used in order to limit as far as possible the DC bus current ripples in order to limit resonance excitation. Since damping coefficient is very close to zero in a high efficiency DC grid, the zero-sequence current which must be introduced in the load has a small amplitude and as a consequence, the auxiliary leg can be designed with low

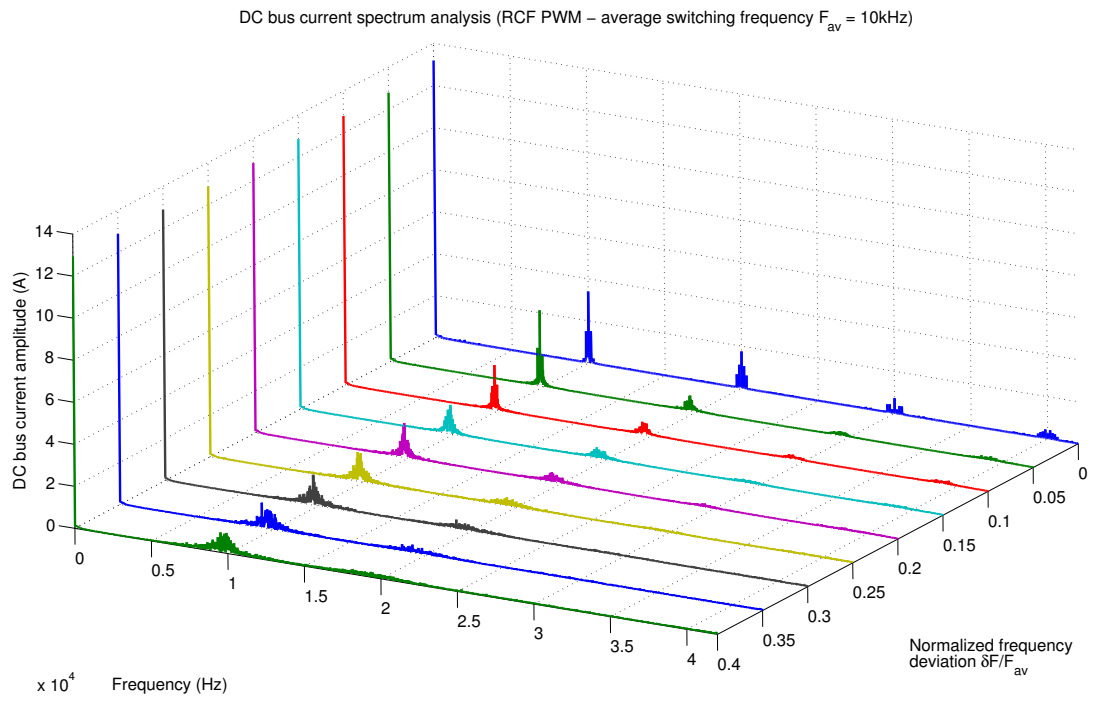


Figure 4: DC current spectrum analysis with RCF PWM

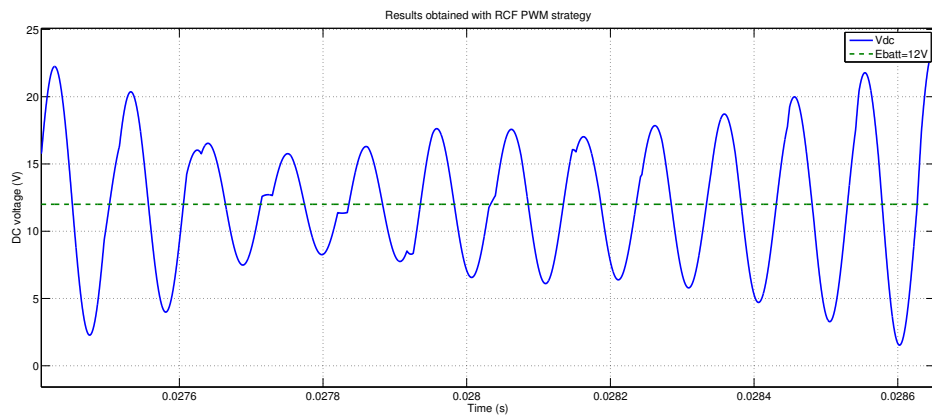


Figure 5: DC voltage waveform

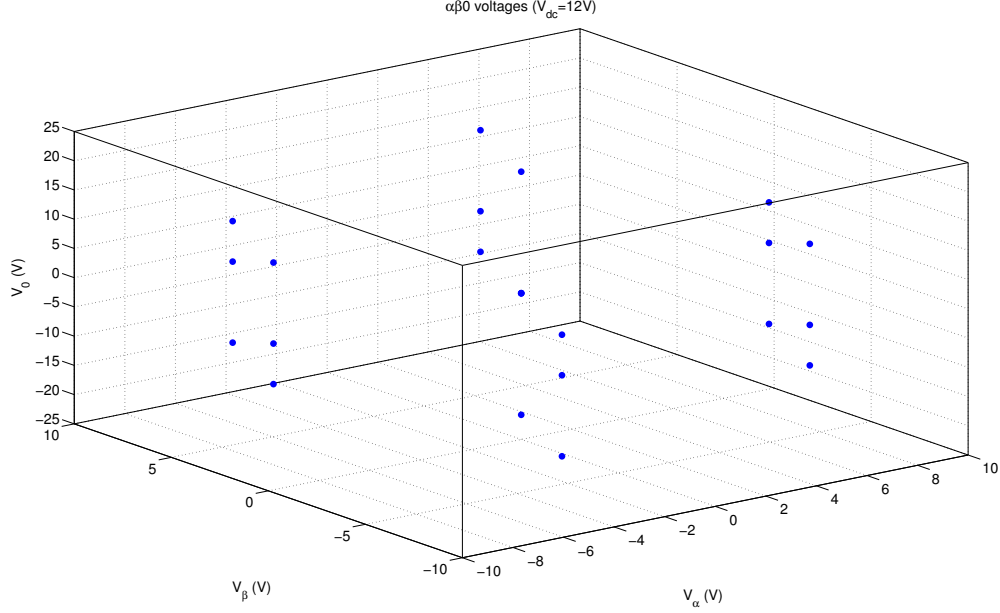


Figure 6: Constellation of $\alpha\beta 0$ voltage vectors available with a three-phase four-legged inverter

rate switches as it can be seen in Fig. 8: indeed, zero-sequence current is greatly lower than $\alpha\beta$ components.

The controller proposed here is based on a predictive control scheme which can be described with the following algorithm

1. Acquisition of state vector components at the beginning of the current sampling period,
2. Prediction of state vector variations on a given time interval T_s for each inverter inputs combinations ($2^4 = 16$ for a three-phase four-legged inverter),
3. Choice of the optimal inverter inputs vector (for a given criterion defined below),
4. Application of this inverter inputs vector during a sampling period T_s ,
5. *Predictions can be possibly verified after this sampling period in order to detect faults for instance (fault-tolerant control).*

The state vector predictions are limited here to $\alpha\beta 0$ currents in the three-phase load. Indeed, it is assumed that DC bus voltage variations are significantly limited by the proposed strategy. Thus, predictions are performed on the basis of this hypothesis ($v_{dc} = V_{dc} = C^{te}$):

$$\begin{cases} i_{\alpha\beta}^{\#}[n+1] = i_{\alpha\beta}^{meas}[n] + \frac{T_s}{L_{\alpha\beta}} (v_{\alpha\beta} - R \cdot i_{\alpha\beta}^{meas}[n]) \\ i_0^{\#}[n+1] = i_0^{meas}[n] + \frac{T_s}{L_0} (v_0 - R \cdot i_0^{meas}[n]) \end{cases} \quad (6)$$

where $x^{\#}[n+1]$ quantities are predicted values of x quantities at $(n+1)^{th}$ sampling instant and $x^{meas}[n]$ is the measurement of quantities at the n^{th} sampling instant (T_s being the sampling period). Then, the $\alpha\beta 0$ inverter output voltages are calculated according to equation (2) and i_{dc} current can be also predicted on the basis of (3) and (6). Finally, the criterion which is optimized (*i.e.* minimized) by the proposed controller is defined as follows:

$$J(i_{\alpha\beta}^{ref}[n+1], i_{\alpha\beta}^{\#}[n+1], i_0^{\#}[n+1]) = \left(\begin{array}{l} \Delta i_{\alpha\beta}[n+1]^t \cdot \Delta i_{\alpha\beta}[n+1] \\ + \lambda \cdot \left(\left(\langle i_{dc} \rangle - i_{dc}^{\#}[n+1] \right) \right)^2 \end{array} \right) \quad (7)$$

¹A normalized amplitude noted $k_m \leq 1$ (overmodulation occurs when $k_m > 1$).

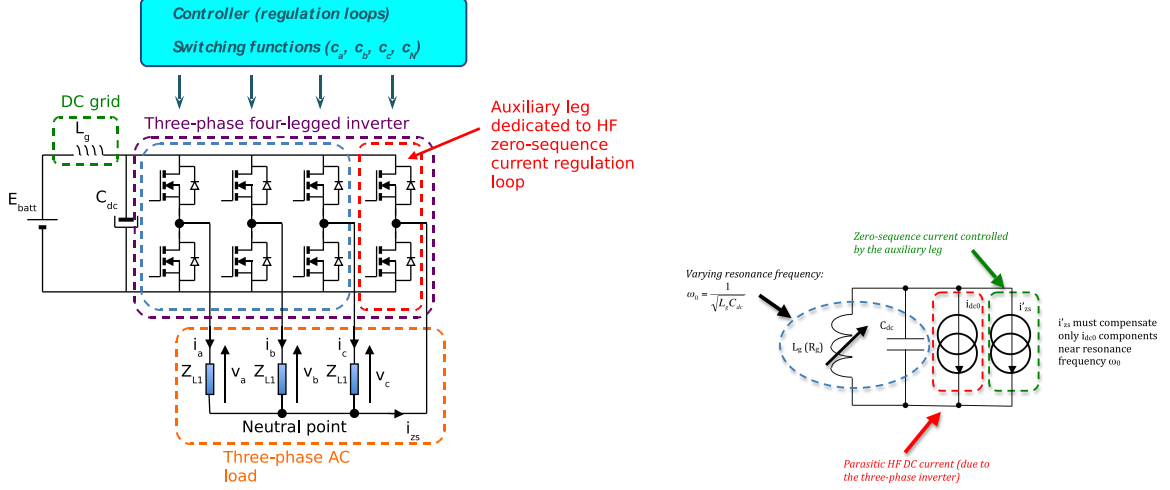


Figure 7: Architecture based on a three-phase four-legged inverter (left) and Four-legged inverter based DC voltage stabilization principle (right)

where

$$\Delta i_{\alpha\beta} = i_{\alpha\beta}^{ref}[n+1] - i_{\alpha\beta}^\# [n+1] \quad (8)$$

and where $i_{\alpha\beta}^{ref}[n+1]$ is the $\alpha\beta$ currents vector reference calculated by an outer regulation loop (speed and/or position). Finally, λ is a tuning parameter which allows to mitigate the i_{dc} variations around its average value.

4.2 Simulation results

Simulations results given in Fig. 7 are obtained with $\lambda = 0.01$. In this case, the DC link voltage is maintained in a very thin interval around 12V. Thus, this topology of converter associated to a predictive controller behaves as an active filter (within a DC bus). Moreover, it can be seen in this figure that the amplitude of the zero-sequence current is greatly lower than the $\alpha\beta$ components. Thus, switches of the auxiliary leg can be at a lower rate than other ones.

5 Conclusion

In this paper, disturbances induced by high frequency switching currents on the DC bus of an inverter have been described in the context of embedded systems such as electric and/or hybrid vehicles. The modeling of the inverter and the DC grid has been detailed in order to highlight the resonance phenomenon and the great variations of the resonance frequency due to parameters uncertainties. Consequently, an adapted control strategy must be applied in order to avoid failures in such a structure. It has been shown that a spread-spectrum PWM strategy (using random carrier frequency) cannot satisfy constraints mainly because of the low damping coefficient of the LC equivalent circuit introduced by DC bus capacitors and DC link inductance. Finally, a three-phase four-legged inverter associated to a predictive control strategy is used in order to introduce a zero-sequence current which is able to compensate the AC component of i_{dc} leading to a dramatic reduction of DC voltage ripples.

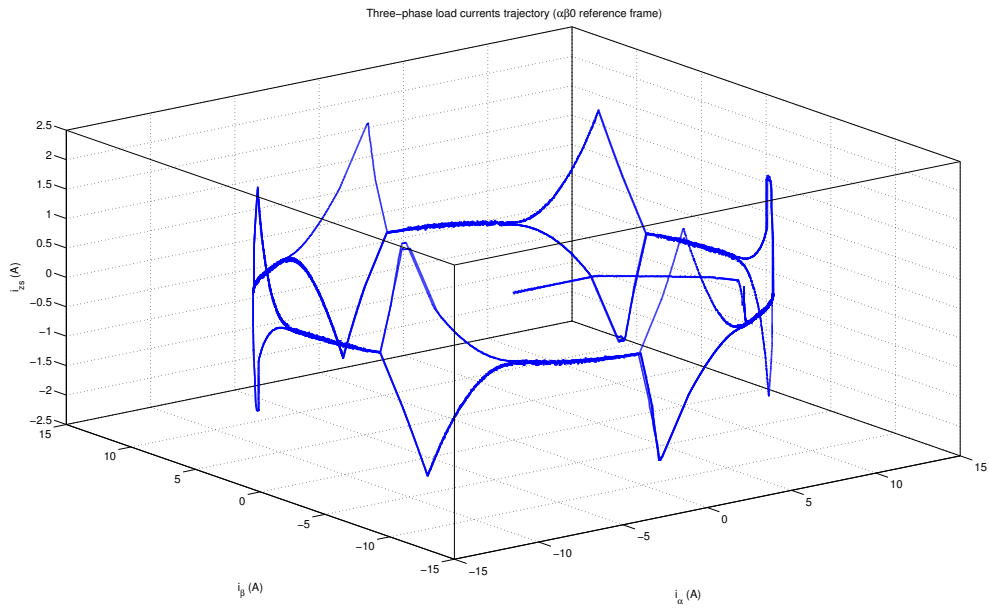


Figure 8: Three-phase currents in $\alpha\beta 0$ reference frame (left) and corresponding DC bus voltage (right)

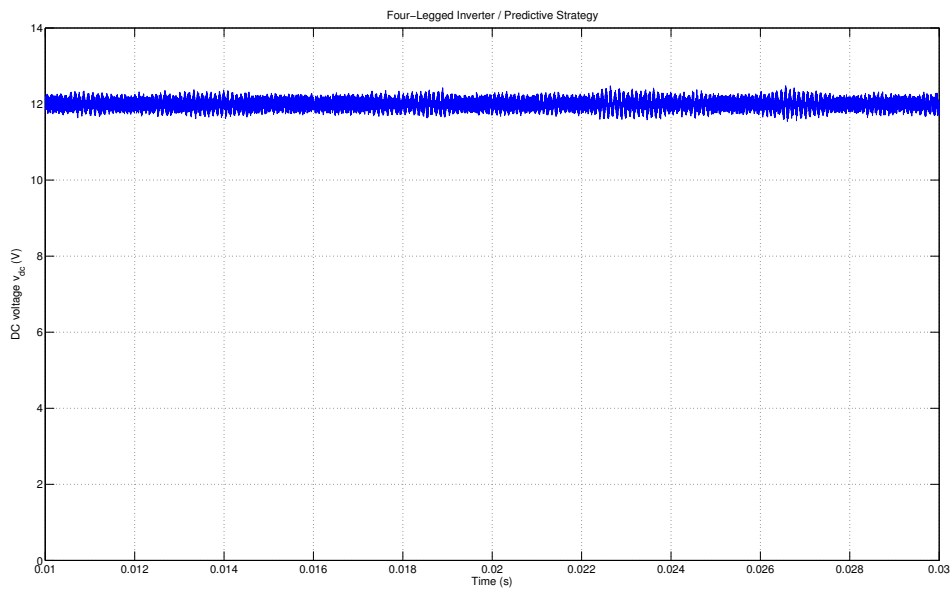


Figure 9: Three-phase currents in $\alpha\beta 0$ reference frame (left) and corresponding DC bus voltage (right)

References

- [1] C.C. Chan, Y.S Wong, The state of the art of electric vehicles technology, in Proc. of the 4th International Power Electronics and Motion Control Conference, 2004. IPEMC 2004. Vol. 1, pp. 46 - 57, 14-16 Aug. 2004, Xi'an, China.
- [2] J. Hobraiche, J.-P. Vilain, C. Plasse, Offline optimized pulse pattern with a view to reducing DC-link capacitor application to a starter generator, in Proc. of IEEE 35th Annual Power Electronics Specialists Conference, PESC04, Vol. 5, pp. 3336 - 3341, 20-25 June 2004, Aachen, Germany.
- [3] A. Stone, B. Chambers, D. Howe, Random carrier frequency modulation of PWM waveforms to ease EMC problems in switched mode power supplies, in Proc. of International Conference on Power Electronics and Drive Systems, Vol. 1, pp. 16-21, 21-24 Feb. 1995, Singapore.
- [4] G. S. Thandi, R. Zhang, K. Xing, F. C. Lee, D. Boroyevich, Modeling, Control and Stability Analysis of a PEBB based DC DPS, IEEE Trans. on Power Delivery, Vol. 14, No. 2, pp. 497-505, Apr. 1999.